

Appearance energies of singly, doubly, and triply charged coronene and corannulene ions produced by electron impact

S. Denifl^a, B. Sonnweber^a, J. Mack^b, L.T. Scott^b, P. Scheier^a, K. Becker^{c,d}, T.D. Märk^{a,*}

^a *Institut für Ionenphysik, Leopold-Franzens Universität, Technikerstrasse 25, A-6020 Innsbruck, Austria*

^b *Merkert Chemistry Center, Boston College, 2609 Beacon Street, Chestnut Hill, MA 02467, USA*

^c *Department of Physics and Engineering Physics, Stevens Institute of Technology, Hoboken, NJ 07030, USA*

^d *Center for Environmental Systems, Stevens Institute of Technology, Hoboken, NJ 07030, USA*

Received 28 October 2005; received in revised form 2 December 2005; accepted 2 December 2005

Available online 18 January 2006

Abstract

Electron impact ionization near threshold has been studied for the polyaromatic hydrocarbons coronene and corannulene using a high resolution electron monochromator in conjunction with quadrupole mass spectrometry. The mass spectra determined at an electron energy of 100 eV show a rich fragmentation pattern (particularly for coronene) including the presence of multiply charged molecular cations for both compounds. For the singly and multiply charged parent ions of coronene and corannulene we present the ionization efficiency curves near threshold from which the corresponding appearance energies (AEs) are determined using a nonlinear least squares fitting routine. The AEs obtained here are compared where available with previous values reported for both compounds using electron impact ionization and photoionization as well as with theoretical predictions.

© 2006 Elsevier B.V. All rights reserved.

Keywords: Electron impact ionization; Appearance energy; Polyaromatic hydrocarbon; Multiply charged ion

1. Introduction

Coronene and corannulene (see Fig. 1 for the molecular structures [1] with optimized geometry using the B3LYP/6-311G** method) belong to the class of large polycyclic aromatic hydrocarbons (PAHs). PAHs play an important role in environmental applications because of their appearance as abundant by-products in the combustion of organic materials [2,3]. Certain members of this family are known for their toxicity [3], and others (neutral and ionized) have been tentatively identified as a source of infrared emission from interstellar matter [4–6]. Coronene is considered to be one of the most representative PAHs in the interstellar space [6]. Moreover, the two PAH compounds coronene (C₂₄H₁₂) and corannulene (C₂₀H₁₀) are of particular interest as they represent a prototype of bowl-shaped (corannulene) and planar PAHs (coronene). Coronene, a particularly stable compound, consists of seven benzene rings. The

molecule is absolutely flat and resembles a layer of graphite. Thus it is considered as a model system for graphite as it possesses the local six-fold symmetry of graphite [7]. Corannulene has a curved-surface structure and is often referred to as a “buckybowl” molecule as it represents the “polar cap” or 1/3 of a C₆₀ fullerene or “buckyball” molecule [8]. Corannulene was first synthesized in 1966 by a difficult 17-step synthesis [9]. In the early 1990s, however, one of our groups developed a much shorter synthesis of corannulene using flash pyrolysis [8].

The ionization of PAHs has received some attention in the literature [10,11], particularly in the context of extensive studies of the ionization energies (IEs) of singly and multiply charged fullerene and fullerene fragment ions [12–15]. In general, the possibility to form multiply charged polyatomic molecular ions is strongly dependent on the properties of the molecule. In most cases the Coulomb repulsion limits the detection of multiply charged ions [16]. Doubly and triply charged (small) molecular ions were obtained experimentally [16]. Exceptional stability was observed for the fullerene C₆₀ cluster where charge states up to 12 were detected experimentally [17]. Ionization energies of the C₆₀ parent cations were reported previously up to charge state $z = 4$ [13] and for C₇₀ up to $z = 6$ [15]. These studies revealed that

* Corresponding author. Also adjunct professor at: Dept. Plasmaphysics, Univerzita Komenského, Mlynska dolina, SK-84248 Bratislava Slovak Republic. Tel.: +43 512 507 6240; fax: +43 512 507 2932.

E-mail address: Tilmann.Maerk@uibk.ac.at (T.D. Märk).

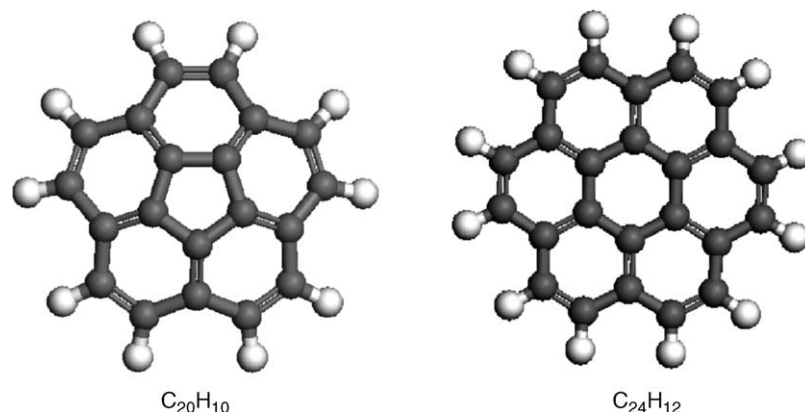


Fig. 1. Molecular structure of corannulene ($C_{20}H_{10}$) and coronene ($C_{24}H_{12}$) with optimized geometry using the B3LYP/6–311G** method [1].

the ionization energies for both fullerenes cations and the same charge state are approximately the same [13]. Another experimental observation was that the ionization energies of fullerenes depend nearly linearly on the charge state [15,18], which was in good agreement with theoretical predictions [19] and with the simple molecular capacitor scaling law of Smith [20]. The latter classical model should also be applicable for fragments of graphite and large PAHs [20].

The IEs of coronene and corannulene were determined in several previous studies [10,11,20–31]. One of the most recent experimental studies was carried out by Schröder et al. [10] who studied single and double ionization of both molecules with three different experimental techniques (including photoionization) combined with *ab initio* theory. In the NIST data base [23] several values for the ionization energy of coronene are listed (in addition to the mass spectrum recorded at the electron energy of 70 eV) which were determined via photoelectron spectroscopy [24,25], electron impact ionization [21,26], gas phase ion-equilibrium studies [27] and measurements of charge transfer spectra [28]. Moreover, a few theoretical studies were dedicated to the determination of the ionization energy of coronene [20,29–31]. Another remarkable experiment not included in NIST was carried out by Tobita et al. [22] who determined single and double ionization potentials of 21 PAHs utilizing photoionization. The ionization energies for singly and doubly charged coronene by means of electron impact were only reported by Gallegos [21]. For corannulene no data is available at the NIST data base. However, in addition to Schröder et al. [10], ionization energies of corannulene were determined by Seiders et al. [11] using photoelectron spectroscopy, UV charge transfer bands and *ab initio* calculations.

The IEs of coronene by means of electron impact reported in 1968 [21] differ strongly with recent photoionization values [10] (e.g., about 0.4 eV for $C_{24}H_{12}^+$ and 2.5 eV for $C_{24}H_{12}^{2+}$; see also Table 1, where the previously reported IEs are listed). Moreover, for corannulene no IEs determined by means of electron impact are available. Here, we report the results of a high resolution electron impact ionization study aimed at the determination of the ionization energies of singly and multiply charged ions of coronene and corannulene under controlled experimen-

tal conditions. The results along with their error margins are compared with other data available in the literature.

2. Experimental technique and data analysis

The experimental apparatus and the data analysis procedure have been described in detail in previous publications [32–34]. Briefly, we use a high-resolution hemispherical electron monochromator in conjunction with a quadrupole mass spectrometer. The molecular target gas beam of coronene or corannulene is produced in a Knudsen type oven originally used for the evaporation of C_{60} . The oven is heated resistively and can reach temperatures up to 800 °C. The yellow coronene-powder has a stated purity of 99% and was purchased from Sigma–Aldrich. Corannulene is not commercially available but was prepared [8] by Mack and Scott for the present experiment. For the crystalline corannulene granulate an oven temperature of about 130 °C is used whereas coronene is heated up to temperatures of about 200 °C for a sufficiently intense molecular beam. The temperature is measured with a Pt100 temperature sensor mounted directly at the oven. Through a capillary with the diameter of 1 mm the gaseous molecules effuse directly into the collision chamber of the hemispherical electron monochromator, where the interaction with the monochromatized electron beam takes place. Previously a maximum electron energy resolution of 35 meV was achieved with the presently used electron monochromator [35]; however, in order to achieve sufficient ion yield, the energy resolution is kept at a value of about 150 meV for the present measurements. The electron energy distribution is determined by the measurement of the s-wave electron attachment reaction to SF_6 or CCl_4 [36,37]. The anion yields of SF_6^-/SF_6 and Cl^-/CCl_4 exhibit a sharp 0 eV peak and the full width at half maximum is a measure of the energy resolution. The cations formed by electron impact ionization of coronene and corannulene are then extracted from the collision chamber by a weak electrostatic field (<20 V/m) and focused into a quadrupole mass spectrometer (maximum mass range 2048 amu). After mass selection the ions are detected by a channeltron type secondary electron multiplier. Using single pulse counting technique the ionization efficiency curve for a selected mass is recorded as a function of the electron energy. For mass

Table 1

Appearance energies for the formation of: (a) $C_{24}H_{12}^{z+}$ ($z = 1-3$), (b) $C_{20}H_{10}^+$ and $C_{20}H_{10}^{2+}$ by electron impact ionization of the respective neutral parent molecule in comparison with other available data utilizing photoionization (PI), theory (C), electron impact (EI), photoelectron spectroscopy (PE), gas phase ion-equilibrium measurements (EQ) and charge transfer spectra (CTS)

Mass (amu)	Ion	AE (eV)	Previous values
(a) Parent molecule: coronene ($C_{24}H_{12}$)			
300	$C_{24}H_{12}^+$	7.40 ± 0.15	7.26 ± 0.05 eV [10] (PI); 6.98 ± 0.20 eV [10] (C (A)); 7.03 ± 0.20 eV [10] (C (V)); 7.65 ± 0.10 [21] (EI); 7.20 ± 0.05 eV [22] (PI); 7.29 eV [24] (PE); 7.34 eV [25] (PE); 7.44 eV [20] (C); 7.50 eV [29] (C); 7.26 ± 0.05 eV [27] (EQ); 7.64 eV [28] (CTS)
150	$C_{24}H_{12}^{2+}$	18.62 ± 0.20	18.50 ± 0.20 eV [10] (PI); 18.7 ± 0.20 eV [22] (PI); 17.77 ± 0.20 eV [10] (C (A)); 17.83 ± 0.20 eV [10] (C (V)); 21.00 ± 0.40 [21] (EI)
100	$C_{24}H_{12}^{3+}$	35.05 ± 0.50	–
(b) Parent molecule: corannulene ($C_{20}H_{10}$)			
250	$C_{20}H_{10}^+$	8.02 ± 0.05	7.83 ± 0.02 eV [10] (PI); 7.58 ± 0.20 eV [10] (C (A)); 7.71 ± 0.20 eV [10] (C (V)); 7.89 eV [11] (PE); 8.37 eV [11] (CTS); 8.77 eV [11] (C)
125	$C_{20}H_{10}^{2+}$	19.83 ± 0.30	20.10 ± 0.20 eV [10] (PI); 19.24 ± 0.20 eV [10] (C (A)); 19.71 ± 0.20 eV [10] (C (V))

Ref. [10] reported calculated adiabatic (A) and vertical (V) values. We note that the present AE values (and the stated margins of uncertainty) are the result of averaging data over several individual measurements.

scans the electron energy is kept constant, and the ion intensity is recorded as a function of the mass. The background pressure in the main chamber is 10^{-6} Pa and is measured with an ionization gauge.

The data analysis is based on a Wannier-type power law for the near-threshold behavior of the cross section for single and multiple ionization [33,38]. Appearance energies are determined from a fit of the measured data sets using the Marquart–Levenberg algorithm (MLA). This is an iterative, non-linear least-squares fitting routine, which we use in conjunction with appropriately selected initial fitting parameters for each data set. In the present cases, where the background signal is essentially constant, we use a 2-function fit to the experimental data of the form:

$$f(E) = b \quad \text{for } E < \text{AE} \quad (1a)$$

$$f(E) = b + c(E - \text{AE})^p \quad \text{for } E > \text{AE} \quad (1b)$$

where b represents the constant background. The constant c denotes the slope of the ion signal above the appearance energy AE and is thus a measure for the intensity of a given ion signal. The exponent p expresses the curvature of the function in the near-threshold region. As demonstrated for rare gases [33,38] and recently also for complex molecules [39], this fitting method allows a reliable and reproducible determination of appearance energies.

3. Results and discussion

3.1. Mass spectra

Fig. 2 shows the mass spectra obtained by 100 eV electron impact on coronene and corannulene. The mass spectrum of coronene (top diagram in Fig. 2) shows many peaks of appreciable intensity indicating a high probability for decomposition upon electron collisions with this molecule. The three peaks of interest for the present study, $C_{24}H_{12}^{z+}$ ($z = 1-3$) are labeled in

the mass spectrum. The doubly charged ion is the most intense peak in the mass spectrum at 100 eV. The mass spectrum shown in Fig. 2 is very different from the coronene mass spectrum shown in the NIST data base [23], which only shows peaks at mass-to-charge ratios corresponding to the singly and doubly charged ion with a dominant parent ion peak (by a factor of 3), but shows no prominent peaks that can be associated with fragments of the molecule. The difference to the NIST data base [23], which were measured at the impact energy of 70 eV, can be explained most likely by the difference in electron energy,

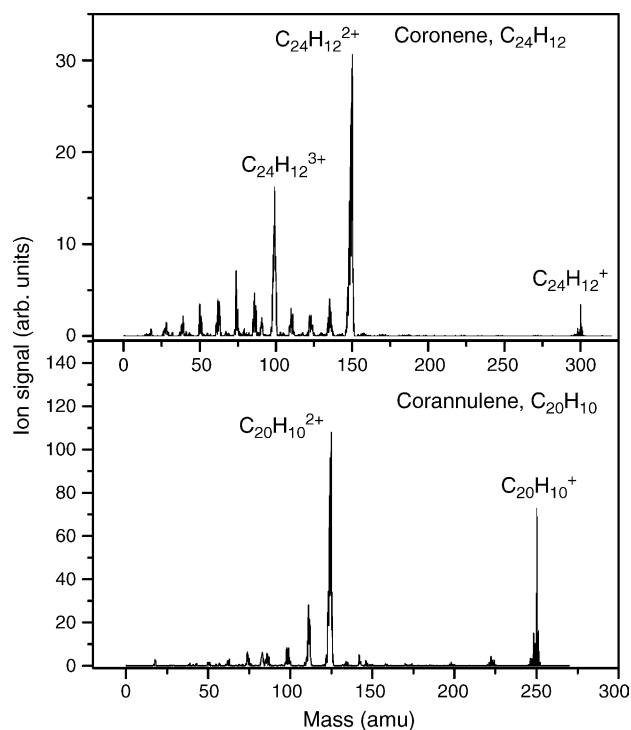


Fig. 2. Mass spectrum of coronene ($C_{24}H_{12}$) (top) and corannulene ($C_{20}H_{10}$) (bottom) recorded at the electron energy of 100 eV. The peaks of the singly and multiply charged molecular ions are labeled.

the different mass dependent detection efficiencies of the setups used and are also due to discrimination effects caused by significant excess kinetic energies of the fragment cations formed via dissociative ionization. We also observed a rather prominent peak at the mass of 75 amu which would indicate the presence of the quadruply charged parent cation $C_{24}H_{12}^{4+}$. However, the measured AE for the cation at this mass contradicts this assignment (see below). The bottom diagram in Fig. 2 shows the mass spectrum of corannulene at an electron energy of 100 eV. This spectrum shows fewer prominent ion peaks compared to coronene and is dominated by the $C_{20}H_{10}^+$ and $C_{20}H_{10}^{2+}$ ion peaks. The presence of fragment cations and the generally rather low intensity of corannulene cations prevent a clear identification of higher charge states of the parent cation. We did not find any mass spectrum of this molecule in the literature.

Please note that the mass spectra shown in Fig. 2 were measured at a mass resolution which also allowed the detection of masses close to the parent cations. However, this adjustment of the quadrupole led to a poor mass resolution for lighter masses. For the measurement of the ionization efficiency curve for a cation below 200 amu, the quadrupole was operated at a higher mass resolution in order to avoid any contamination by other ions.

3.2. Ionization efficiency curves

Subsequently, the mass spectrometer was used to select a particular ion and near-threshold electron energy scans were obtained by repeatedly ramping the electron energy over a pre-determined energy interval and recording the ion signal as a function of the electron energy. Fig. 3 shows the ion signals as a function of the electron energy for the formation of singly, doubly, and triply charged coronene ions in the near-threshold region. The fit shown in the diagrams and the extracted appearance energy, derived via the fitting procedure described in Section 2, are shown in each diagram. The appearance energies extracted from our measured data sets for the formation of $C_{24}H_{12}^{z+}$ ($z = 1-3$), $C_{20}H_{10}^+$ and $C_{20}H_{10}^{2+}$ are summarized in Table 1 and are compared to other available data for coronene and corannulene [10,11,20–22,24,25,27–29]. We note that the AE values (and the stated margins of uncertainty) in Table 1 are the result of averaging data of up to five individual measurements carried out on different days. The error margins listed in Table 1 are significantly larger than the uncertainty based on the statistical level of confidence of a fit to a single data set. Where error margins are given by other authors, these errors refer to the error margins quoted in the original publications.

The single photoionization [10,22] of coronene requires about 200 meV less than the electron impact ionization in our experiment, a phenomenon frequently encountered if high resolution electron and photon experiments are compared [32,40]. In accordance with previous studies [32,40] we interpret this as a signature of different ionization mechanisms for these two different ionizing agents. The only previous values for the singly charged coronene cation using electron impact were reported by Gallegos [21] and Gallegos et al. [26] measured with a standard mass spectrometer. The reported AE for the parent cation

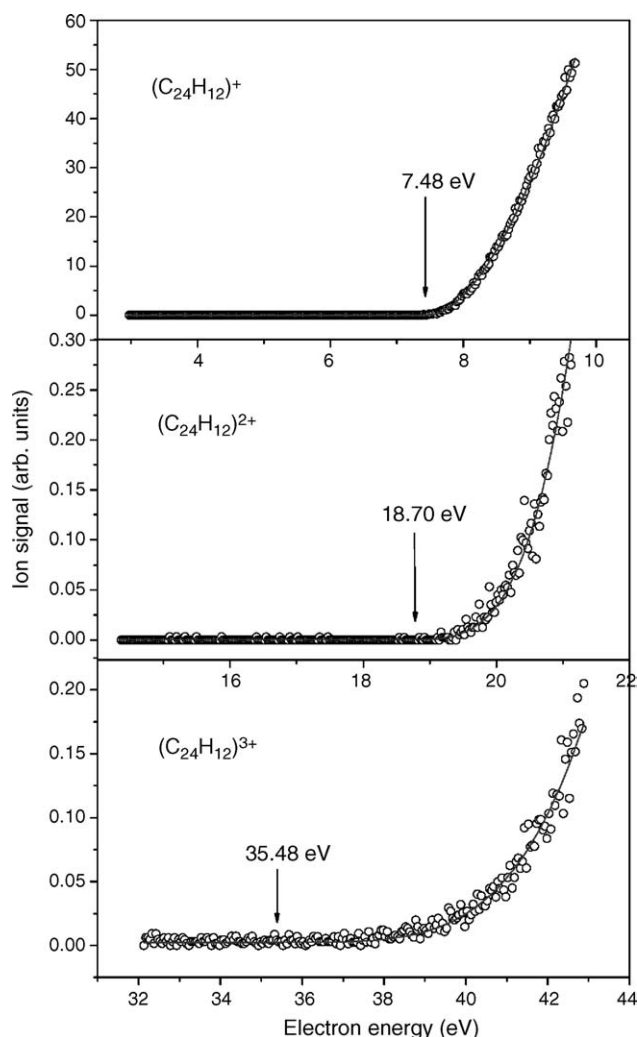


Fig. 3. Threshold ionization efficiency curves (open circles) of the singly (top), doubly (middle) and triply (bottom) charged coronene cation, respectively. The fit curves are shown as solid lines. The AEs indicated by arrows are the thresholds for these individual data sets and differ from the AEs given in the text and in the table which are derived by averaging several AE values from individual data runs.

(7.65 ± 0.10 eV [21] and 7.68 ± 0.05 eV [26], respectively) is in fair agreement with the present value (7.40 ± 0.15 eV). However, the AE for the doubly charged coronene reported by Gallegos [21] (21.00 ± 0.40 eV) exceeds our measured AE by 2.38 eV. In contrast, previous photoionization studies [10,22] yielded a double ionization potential of coronene which is close to the present AE of 18.62 ± 0.20 eV. Tobita et al. [22] reported a value of 18.70 ± 0.20 eV and Schröder et al. [10] reported a value of 18.50 ± 0.20 eV. In previous photoelectron studies, a slightly lower ionization energy of coronene was observed (7.29 eV [24] and 7.34 eV [25]). Moreover, the single ionization potential of coronene was determined via gas phase ion-equilibrium measurements [27], charge transfer spectra [28] and also obtained from theoretical calculations [20,29–31] and values in the range from 7.26 to 7.64 eV were observed (for a complete overview, see [23,21]). We were also able to determine the AE of triply charged coronene which has a threshold of 35.05 ± 0.50 eV. No previous values are reported in literature for this case.

Similar scans were carried out for $\text{C}_{20}\text{H}_{10}^+$ and $\text{C}_{20}\text{H}_{10}^{2+}$, which are not shown here. The corresponding average AE values derived from these data sets are included in Table 1. The present AE value for $\text{C}_{20}\text{H}_{10}^+$ (8.02 ± 0.05 eV) is again about 200 meV higher than the photoionization value reported by Schröder et al. [10]. Similar value like in photoionization was obtained via photoelectron spectroscopy ($\text{IE}(\text{C}_{20}\text{H}_{10}^+) = 7.89$ eV) [11] in contrast to the value derived via charge transfer spectra ($\text{IE}(\text{C}_{20}\text{H}_{10}^+) = 8.37$ eV) [11]. Theoretical calculations performed in these two previous studies [10,11] differ strongly by more than 1 eV. Seiders et al. observed an ionization energy of 8.77 eV for corannulene using the $\Delta(\text{SCF})$ method at the MP2/cc-pVDZ// MP2/cc-pVDZ level of theory [11]. Schröder et al. [10] calculated adiabatic and vertical ionization energies at the B3LYP/6–311G(d, p) level of theory with an estimated accuracy of 0.2 eV. They observed values of 7.58 ± 0.20 and 7.71 ± 0.20 eV for $\text{C}_{20}\text{H}_{10}^+$, respectively, i.e., adiabatic and vertical ionization energy show a stronger spread than in the case of coronene (see Table 1). The same calculations were also performed for the doubly charged corannulene parent cation. In that case, values of 19.24 ± 0.20 and 19.71 ± 0.20 eV were reported for the adiabatic and vertical ionization energy, respectively [10]. The double ionization energy of corannulene observed in the photoionization experiment was 20.10 ± 0.20 eV [10]. Thus, taking also into account the results for coronene, Schröder et al. concluded that their calculations slightly underestimate the adiabatic ionization energy compared with their experimental results.

According to Smith [20], large polyaromatic hydrocarbons like coronene and corannulene ionize like fragments of graphite, i.e., the ionization potentials approach the sum of the graphite work function and the electrostatic work for charging a conductor of the size and shape of the aromatic hydrocarbon. This classical model can be used to predict molecular-size-dependent single ionization energies as well as multiple ionization energies. In this approximation, the molecule is treated as a charged circular conducting disk bounded by the peripheral carbon skeleton of the aromatic system [20]. The ionization process occurs in two steps: (i) the electron is raised to the vacuum level and (ii) the electron is removed to infinity from the conducting plate with radius R . The z th ionization potential can then be calculated by the following equation [20]:

$$\text{IE}_z = zV + z^2U \quad (2)$$

where IE_z is the energy to ionize the PAH z times, V the work function and U denotes the specific capacitive potential. The work function V is very close to the work function of graphite. Assuming the same work function as for graphite, Smith calculated the single ionization potential for coronene to be 7.44 eV [20]. Taking into account the simplicity of the model, this value is in good agreement with the present experimental AE value. Using Eq. (2), it is also possible to predict the IP of higher charged hydrocarbons from known IPs for two different charge states. Using our experimental AEs for the singly and doubly charged coronene in (2), we can determine V ($=5.49$ eV) and U ($=1.91$ eV) for coronene. For $z=3$ in Eq. (2), we determine

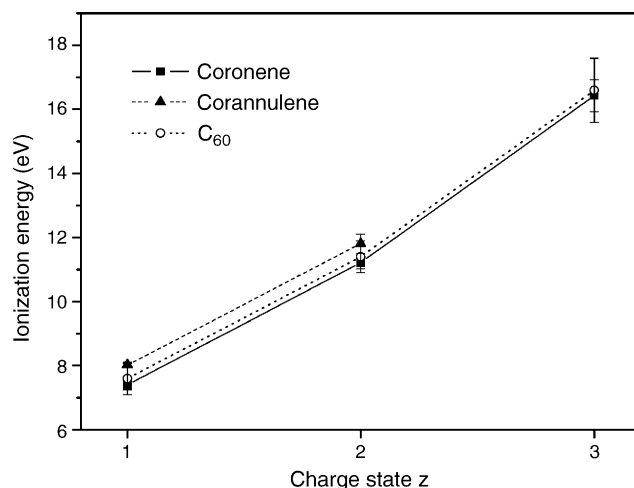


Fig. 4. Ionization energy (eV) vs. final charge state z for parent cations of coronene (full squares and full line), corannulene (full triangles and dashed line) and of C_{60} (open circles and dotted line) taken from [13]. Also included in the figure are the corresponding error bars.

an $\text{AE}(\text{C}_{24}\text{H}_{12}^{3+})$ of 33.66 eV which is in fair agreement with our measured AE (35.05 ± 0.50 eV). For a comparison with the predicted nearly linear dependence of the ionization energy on the initial charge state, we plotted our values for the singly and multiply charged coronene and corannulene cations as a function of the final charge state which is shown in Fig. 4. Also included in this figure are the ionization energies of C_{60} taken from [13]. Within the error bars of the experimental values, we observe a nearly linear dependence of the ionization energy with increasing charge state. Moreover, coronene, corannulene and C_{60} appear to have exactly the same dependence upon multiple ionization.

We also measured the ionization efficiency at mass 75 amu, i.e., the mass of the quadruply charged coronene parent cation ($\text{C}_{24}\text{H}_{12}^{4+}$). Applying the model of Smith [20], one derives a threshold for $\text{C}_{24}\text{H}_{12}^{4+}$ of 52.52 eV. Our experimentally determined value for the cation is 40.07 ± 0.60 eV, i.e., it strongly deviates from the nearly linear increase of the AE with increasing charge state. Thus, we assign this threshold to the formation of a fragment cation (e.g., C_6H_3^+) and not to $\text{C}_{24}\text{H}_{12}^{4+}$.

In conclusion, the detection efficiency of our crossed electron neutral beams apparatus allows us to determine the appearance energies of multiply charged coronene (up to $z=3$) and corannulene (up to $z=2$). From the present results, a few tendencies concerning the multiple ionization of coronene and corannulene can be deduced: (i) the present AEs are lower than the previous (less accurate) values observed in electron impact ionization experiments by Gallegos [21] (the differences are 250 meV for $z=1$ and 2.38 eV for $z=2$, respectively), (ii) single photoionization requires slightly less energy (about 200 meV) than electron impact ionization which is not the case for double ionization, (iii) the vertical ionization energies for single and double ionization calculated by Schröder et al. [10] are about 120–800 meV lower than our experimental values, (iv) good agreement is observed between the present results and the simple classical molecular capacitor model by Smith [20], (v) except for a small differ-

ence in the absolute value of the (multiple) ionization energy, coronene and corannulene show the same behavior upon multiple ionization like C₆₀, i.e., a nearly linear dependence of the ionization energy from the charge state.

Acknowledgements

This work has been supported by the FWF, Wien, Austria, the European Commission, Brussels, and the U.S. Department of Energy and NASA.

References

- [1] S. Denifl, S. Ptasíńska, B. Sonnweber, P. Scheier, D. Liu, F. Hagelberg, J. Mack, L.T. Scott, T.D. Märk, *J. Chem. Phys.* 123 (2005) 104308.
- [2] R.I. Freudental, P.W. Jones (Eds.), *Polynuclear Aromatic Hydrocarbons*, Raven Press, New York, 1976.
- [3] J. Ahrens, A. Keller, R. Kovacs, K.-H. Homann, *Ber. Bunsen-Ges. Phys. Chem.* 102 (1998) 1823.
- [4] J.M. Schulmann, R.L. Disch, *J. Phys. Chem. A* 101 (1997) 9176.
- [5] S.R. Langhoff, *J. Phys. Chem.* 100 (1996) 2819.
- [6] A. Omont, *Astron. Astrophys.* 164 (1986) 159.
- [7] A.M. Orendt, J.C. Facelli, S. Bai, A. Rai, M. Gossett, L.T. Scott, J. Boerio-Goates, R.J. Pugmire, D.M. Grant, *J. Phys. Chem. A* 104 (2000) 149.
- [8] L.T. Scott, P.-C. Cheng, M.M. Hashemi, M.S. Bratcher, D.T. Meyer, H.B. Warren, *J. Am. Chem. Soc.* 119 (1977) 10963, and references cited therein.
- [9] W. Barth, R. Lawton, *J. Am. Chem. Soc.* 88 (1966) 380.
- [10] D. Schröder, J. Loos, H. Schwarz, R. Thiessen, D.V. Preda, L.T. Scott, D. Caraiman, M.V. Frach, D.K. Böhme, *Helv. Chim. Acta* 84 (2001) 1625.
- [11] T.J. Seiders, K.K. Baldrige, J.S. Siegel, R. Gleiter, *Tetrahedron Lett.* 41 (2000) 4519.
- [12] P. Scheier, B. Dünser, R. Wörgötter, M. Lezius, R. Robl, T.D. Märk, *Int. J. Mass Spectrom. Ion Proc.* 138 (1994) 77.
- [13] R. Wörgötter, B. Dünser, P. Scheier, T.D. Märk, *J. Chem. Phys.* 101 (1994) 8674.
- [14] P. Scheier, T.D. Märk, *Int. J. Mass Spectrom. Ion Proc.* 146/147 (1995) 233.
- [15] S. Matt, O. Echt, R. Wörgötter, V. Grill, P. Scheier, C. Lifshitz, T.D. Märk, *Chem. Phys. Lett.* 264 (1997) 149.
- [16] D. Schröder, H. Schwarz, *J. Phys. Chem. A* 103 (1999) 7385.
- [17] V.R. Bhardwaj, P.B. Corkum, D.M. Rayner, *Phys. Rev. Lett.* 91 (2003) 203004.
- [18] H. Steger, J. Holzapfel, A. Hielscher, W. Kamke, I.V. Hertel, *Chem. Phys. Lett.* 234 (1994) 455.
- [19] C. Yannouleas, U. Landmann, *Chem. Phys. Lett.* 217 (1994) 175.
- [20] F.T. Smith, *J. Chem. Phys.* 34 (1961) 793.
- [21] E.J. Gallegos, *J. Phys. Chem.* 79 (1968) 3452.
- [22] S. Tobita, S. Leach, H.W. Jochims, E. Illenberger, H. Baumgärtel, *Can. J. Phys.* 72 (1994) 1060.
- [23] NIST Chemistry WebBook. <http://webbook.nist.gov/chemistry>.
- [24] E. Clar, J.M. Robertson, R. Schlogl, W. Schmidt, *J. Am. Chem. Soc.* 103 (1981) 1320.
- [25] R. Boschi, W. Schmidt, *Tetrahedron Lett.* 25 (1972) 2577.
- [26] E.J. Gallegos, R.F. Klaver, *J. Sci. Instrum.* 44 (1967) 427.
- [27] M. Mautner (Meot-Ner), *J. Phys. Chem.* 84 (1980) 2716.
- [28] H. Koruda, *Nature* 201 (1964) 1214.
- [29] F.A. Matson, *J. Chem. Phys.* 24 (1956) 602.
- [30] N.S. Hush, J.A. Pople, *Trans. Faraday Soc.* 51 (1955) 600.
- [31] E.S. Pysh, N.C. Yang, *J. Am. Chem. Soc.* 85 (1963) 2124.
- [32] M. Probst, K. Hermansson, J. Urban, P. Mach, D. Muigg, G. Denifl, T. Fiegele, N.J. Mason, A. Stamatovic, T.D. Märk, *J. Chem. Phys.* 116 (2001) 984.
- [33] S. Denifl, B. Gstir, G. Hanel, L. Feketeova, S. Matejcik, P. Scheier, K. Becker, A. Stamatovic, T.D. Märk, *J. Phys. B* 35 (2002) 4685.
- [34] G. Hanel, B. Gstir, T. Fiegele, F. Hagelberg, K. Becker, P. Scheier, A. Snegursky, T.D. Märk, *J. Chem. Phys.* 116 (2002) 2456.
- [35] D. Muigg, G. Denifl, A. Stamatovic, T.D. Märk, *Chem. Phys.* 239 (1998) 409.
- [36] S. Matejcik, G. Senn, P. Scheier, A. Kiendler, A. Stamatovic, T.D. Märk, *J. Chem. Phys.* 107 (1997) 8955.
- [37] G. Senn, J.D. Skalny, A. Stamatovic, N.J. Mason, P. Scheier, T.D. Märk, *Phys. Rev. Lett.* 85 (1999) 5028.
- [38] B. Gstir, S. Denifl, G. Hanel, M. Rümmele, T. Fiegele, P. Cicman, M. Stano, S. Matejcik, P. Scheier, K. Becker, A. Stamatovic, T.D. Märk, *J. Phys. B* 35 (2002) 2993.
- [39] S. Denifl, B. Sonnweber, G. Hanel, P. Scheier, T.D. Märk, *Int. J. Mass Spectrom.* 238 (2004) 47, and references cited therein.
- [40] O. Echt, T. Fiegele, M. Rümmele, M. Probst, S. Matt-Leubner, J. Urban, P. Mach, J. Leszczynski, P. Scheier, T.D. Märk, *J. Chem. Phys.* 123 (2005) 084313.